

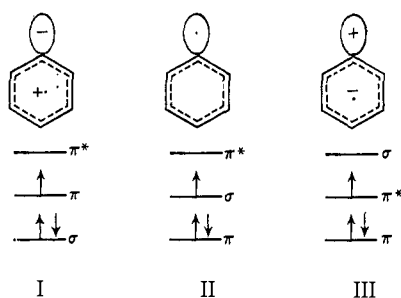
## The Electronic Ground States of Aryl Radicals

Paul H. Kasai, P. A. Clark, and Earl B. Whipple

*Contribution from the Union Carbide Research Institute, Tarrytown, New York 10591. Received November 14, 1969*

**Abstract:** The electronic ground states of phenyl, 1- and 2-naphthyl, 1- and 9-anthracyl, and 1-pyrenyl radicals are determined by means of electron spin resonance in order to find if a crossing of  $\sigma$  and  $\pi$  levels occurs as the aromatic ring system is expanded. In all cases the unpaired electron was found to occupy the essentially nonbonding  $\sigma$  orbital corresponding to the broken bond. Theoretical considerations suggest, however, that the half-occupied orbital may not in fact be uppermost in energy. Proton hyperfine splittings in phenyl and 1- and 2-naphthyl radicals are in good agreement with the results predicted by the theory of Pople, Beveridge, and Dobosh.

When an aryl radical is formed by homolytic cleavage of a peripheral  $\sigma$  bond of a planar arene any one of three situations could result depending on the relative energies of three molecular orbitals concerned. These are depicted in I through III below. The  $\sigma$  orbital



corresponding to the broken bond is sensitive to the local hybridization, while the  $\pi$  orbitals depend primarily on the size and structure of the carbon network.<sup>1</sup> The phenyl radical has been shown to be a  $\sigma$  radical (case II) by Porter and Ward,<sup>2</sup> who investigated its electronic spectrum using a flash photolysis method, by Bennett, Mile, and Thomas,<sup>3</sup> who studied its esr spectrum in various matrices at 77°K, and most recently by Kasai, Hedaya, and Whipple,<sup>4</sup> who made a more detailed analysis of the esr spectrum of the radicals generated and trapped in an argon matrix at 4°K. If the ring system is extended, one would expect that the energy of the  $\sigma$  orbital would not be greatly altered while the energies of the innermost  $\pi$  orbitals would converge asymptotically on the energy of a carbon 2p atomic orbital. This behavior as predicted by simple Hückel theory is illustrated in Figure 1. Unless, therefore, the energy of the nonbonding  $\sigma$  orbital is very close to the limiting  $\pi$ -electron energies one might reasonably expect a crossing of levels as the conjugated network is extended, leading eventually to either case I or case III.

We report here the results of our electron spin resonance studies and molecular orbital calculations of several larger aryl radicals conducted with this particular question in mind. The radicals investigated were 1- and 2-naphthyl radicals, 1- and 9-anthracyl radicals, and 1-pyrenyl radical. The analysis of the spectra led us to conclude that all are  $\sigma$  radicals. In order to fur-

ther elucidate the relative positions of the relevant  $\sigma$  and  $\pi$  orbitals, we then investigated the electronic structures of phenyl, 1- and 2-naphthyl, and 9-anthracyl radicals by means of the extended Hückel molecular orbital theory (EHT).<sup>5</sup> Finally the calculations were repeated for phenyl and  $\alpha$ - and  $\beta$ -naphthyl radicals using the unrestricted self-consistent field method of intermediate neglect of differential overlap (INDO) recently proposed by Pople, Beveridge, and Dobosh.<sup>6</sup>

We shall first describe the observed spectra and their analyses. The discussion of these results and the results of the molecular orbital calculations are presented in the final section.

## Esr Spectra and Analyses

The design of the dewar and the esr spectrometer assembly which allows the trapping of reactive species in rare-gas matrices and the measurements of their esr spectra at 4°K has been described previously.<sup>4,7</sup> As in the case of our study of phenyl radical,<sup>4</sup> all the aryl radicals reported here were generated by the photolysis of the corresponding iodides, trapped in an argon matrix at 4°K, and their esr spectra examined at this temperature. The frequency of the spectrometer locked to the sample cavity was 9.435 GHz. Although it has already been reported in detail we shall begin with a brief description of the phenyl radical spectrum in order to facilitate the understanding of the rest of the spectra. In the following text, we shall adopt the convention that the proton attached to carbon 2, for example, will be called proton 2, etc.

**Phenyl Radical.** Figure 2 shows the spectrum of phenyl radical together with the spectrum simulated, by means of the method described in ref 4, using the  $g$  tensor and the hyperfine coupling tensors given in Table I. The hyperfine coupling interaction with the *para* proton is very small, and the gross features of the spectrum can be described as a triplet of triplets. The larger triplet is ascribed to the coupling to the two *ortho* protons, and the smaller triplet to the coupling to the two *meta* protons. This feature is more evident in the spectrum obtained from *p*-deuteriophenyl radicals as illustrated in Figure 3. The large but extremely anisotropic coupling to the *ortho* protons is strong evidence

(1) The corresponding situation at the edges of graphitic layers has been discussed by C. A. Coulson, "Proceedings of the Fourth Conference on Carbon," Pergamon Press, New York, N. Y., 1960, p 215.

(2) G. Porter and B. Ward, *Proc. Roy. Soc., Ser. A*, **287**, 457 (1965).

(3) J. E. Bennett, B. Mile, and A. Thomas, *ibid.*, **293**, 246 (1966).

(4) P. H. Kasai, E. Hedaya, and E. B. Whipple, *J. Amer. Chem. Soc.*, **91**, 4364 (1969).

(5) R. Hoffmann, *J. Chem. Phys.*, **39**, 1307 (1963).

(6) J. A. Pople, D. L. Beveridge, and P. A. Dobosh, *ibid.*, **47**, 2026 (1967).

(7) P. H. Kasai, E. B. Whipple, and W. Weltner, Jr., *ibid.*, **44**, 2581 (1966).

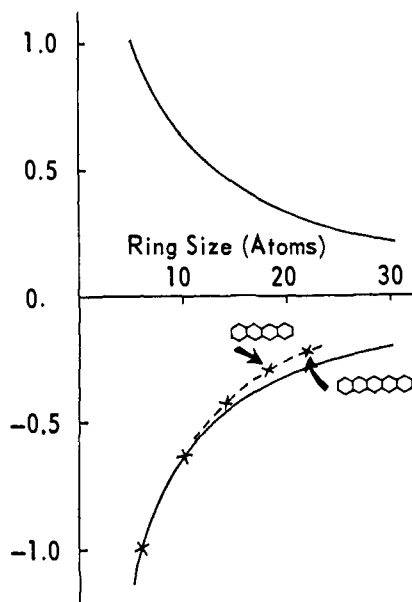


Figure 1. Innermost  $\pi$ -orbital energy (in units of the carbon-carbon exchange integral,  $\beta$ ) vs. size of the conjugated ring. HMO energies of some crosslinked ring systems are also indicated along the broken curve.

for the localization of the unpaired electron in the non-bonding  $\sigma$  orbital created at the broken bond.

**1-Naphthyl Radical.** Lloyed, Magnotta, and Wood produced 1-naphthyl radicals by a novel technique of radioactive decay of tritium in solid naphthalene-1-*t*.<sup>8</sup> They observed an esr spectrum consisting of two

Table I. Assessed Parameters of Phenyl and 2-Naphthyl Radicals<sup>a</sup>

	<i>x</i>	<i>y</i>	<i>z</i>	<i>A</i> (isotropic)
Phenyl Radical				
<i>g</i> tensor <sup>b</sup>	2.0014	2.0023	2.0034	
<i>A</i> ( <i>ortho</i> ) <sup>c</sup>	21.9	15.4	14.9	17.4
<i>A</i> ( <i>meta</i> )	6.6	6.1	5.0	5.9
<i>A</i> ( <i>para</i> )	2.0	2.5	1.2	1.9
2-Naphthyl Radical				
<i>g</i> tensor <sup>b</sup>	2.0014	2.0023	2.0030	
<i>A</i> (H <sub>1</sub> ) <sup>c</sup>	20.1	13.9	13.2	15.7
<i>A</i> (H <sub>3</sub> )	24.1	17.9	17.2	19.7
<i>A</i> (H <sub>4</sub> )	6.4	6.2	4.7	5.8

<sup>a</sup> The *y* axis is parallel to the broken bond and the *z* axis is perpendicular at the molecular plane. <sup>b</sup> The values given for the *g* tensor are accurate to within  $\pm 0.0005$ . <sup>c</sup> Coupling constants are given in gauss and are accurate to within  $\pm 0.1$  G.

broad lines with a separation of 17 G, and attributed the structure to the coupling with proton 2. The esr spectrum obtained by our photolysis technique is shown in Figure 4A. One can recognize, in addition to the doublet feature reported by Lloyed, *et al.*, many additional smaller couplings. If 1-naphthyl radical is also a  $\sigma$  radical, one would expect the magnitudes of the couplings to protons 2, 3, and 4 to be very close to those of the *ortho*, *meta*, and *para* protons in phenyl radical, respectively. As will be shown later, this view is supported by the result of our INDO calculations. The

(8) R. V. Lloyed, F. Magnotta, and D. E. Wood, *J. Amer. Chem. Soc.*, **90**, 7142 (1968).

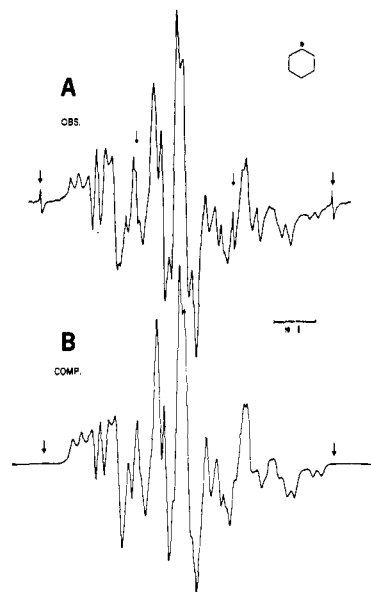


Figure 2. (A) ESR spectrum of phenyl radical in an argon matrix at 4°K. The arrows indicate the quartet due to the methyl radical. (B) Spectrum simulated based upon the assignment given in Table I.

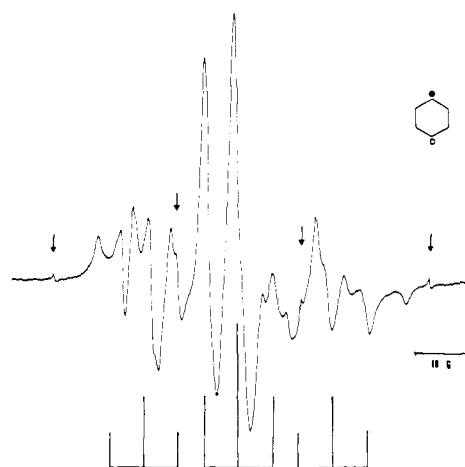


Figure 3. ESR spectrum of *para*-deuterated phenyl radical in an argon matrix at 4°K. Note the triplet-of-triplet pattern arising from the *ortho* and the *meta* protons. The arrows indicate the quartet due to methyl radical.

calculation for 1-naphthyl radical, however, predicted that the isotropic coupling to proton 5 is almost as large as that to proton 4. Thus considering the observed result of phenyl radical, one should expect a coupling of  $\sim 2$  G to both protons 4 and 5. One might also expect a dipolar coupling of about the same magnitude to proton 8. However, based upon the experimental result obtained from 1-pyrenyl radicals which will be discussed later, we believe that the contribution to the hyperfine structure by proton 8 is negligibly small. Thus, most of the detailed structures resolved in Figure 4A are due to the hyperfine interactions with protons 3, 4, and 5. No attempt was made to analyze this structure. Figure 4B is a spectrum simulated borrowing from the observed result of phenyl radical the *g* tensor, the coupling tensors of the *ortho* and *meta* protons for protons 2 and 3, respectively, and assuming a Lorentzian line shape with the line width of 4 G to

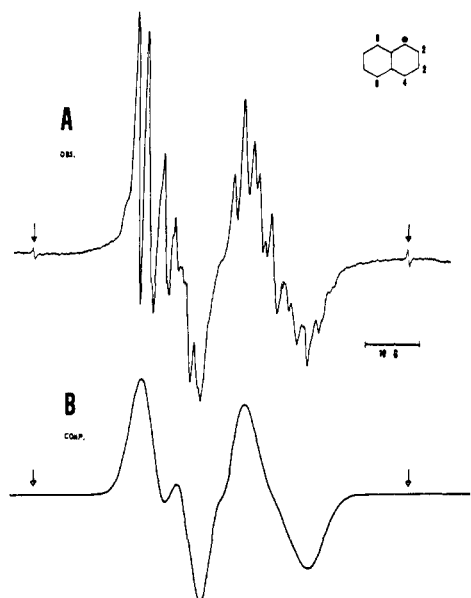


Figure 4. (A) ESR spectrum of 1-naphthyl radical in an argon matrix at 4°K. The arrows indicate the outermost components of the methyl quartet. (B) Spectrum simulated using the  $g$  tensor and the coupling tensors of the *ortho* and *meta* protons of the phenyl radical for protons 2 and 3, and assuming a Lorentzian line shape with the line width of 4 G.

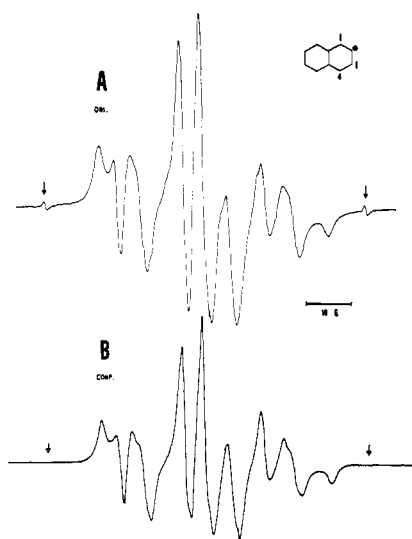


Figure 5. (A) ESR spectrum of 2-naphthyl radical in an argon matrix at 4°K. The arrows indicate the outermost components of the methyl quartet. (B) Spectrum simulated based upon the assignment given in Table I.

approximate the overall effect of the hyperfine coupling interactions with the other protons. Its agreement with the envelop of the observed spectrum clearly indicates the proximity of the nature of the hyperfine interactions in 1-naphthyl radical to that in phenyl radical. We conclude, therefore, that 1-naphthyl radical is a  $\sigma$  radical.

**2-Naphthyl Radical.** The esr spectrum of 2-naphthyl radical is shown in Figure 5A. The overall triplet-of-doublet pattern is what is expected, if the radical is of  $\sigma$  type. The triplet spacing of about 17 G is attributed to protons 1 and 3, while the doublet spacing of about 5 G is assigned to the coupling with proton 4. Based on the proximity of these figures to the coupling constants

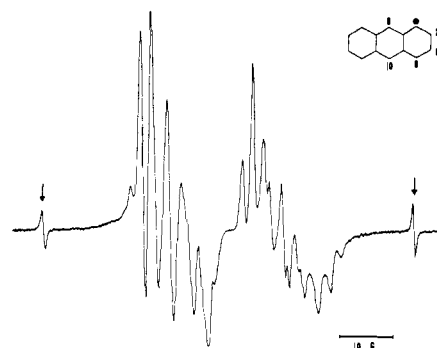


Figure 6. ESR spectrum of 1-anthracyl radical in an argon matrix at 4°K. The arrows indicate the outermost components of the methyl quartet. Note the similarity to the spectrum of 1-naphthyl radical, Figure 4.

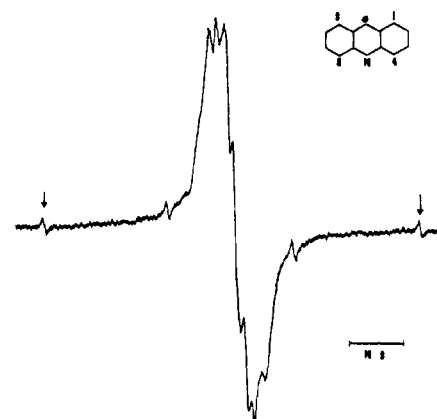


Figure 7. ESR spectrum of 9-anthracyl radical in an argon matrix at 4°K. The arrows indicate the outermost components of the methyl quartet.

with the *ortho* and *meta* protons in phenyl radical, we conclude that 2-naphthyl radical is also a  $\sigma$  radical. A careful analysis of the spectrum revealed, however, that the coupling tensors to protons 1, 3, and 4 assessed by means of the simulation technique are given in Table I. Figure 5B is the spectrum simulated using these parameters. A large difference between the isotropic coupling constants of protons 1 and 3 is surprising. One should note that, on the basis of the available experimental data alone, it is not possible to decide which one of these protons should have a larger coupling constant. The coupling tensor with the largest isotropic coupling constant was assigned to proton 3 based upon the result of the INDO calculation.

**1-Anthracyl Radical.** Figure 6 shows the esr spectrum of 1-anthracyl radical trapped in an argon matrix at 4°K. The similarity of this spectrum to that obtained from 1-naphthyl radical is very striking. One can thus conclude, without further analysis, that 1-anthracyl radical is also of  $\sigma$  type.

**9-Anthracyl Radical.** If 9-anthracyl radical were a  $\pi$  radical, the hyperfine interaction tensors with various protons should be similar to those of the anthracene cation radical. A prominent feature of the anthracene cation radical is a rather large coupling of 6.5 G to protons 9 and 10. The observed esr spectrum of 9-anthracyl radical is shown in Figure 7. It shows no major

hyperfine interaction with any proton. The overall spread of the signal amounts to  $\sim 17$  G and the partially resolved structure suggests small hyperfine interactions ( $\sim 2$  G) with several protons. It thus appears that 9-anthracyl radical is also a  $\sigma$  radical. The small coupling interactions are due to proton 10 and probably protons 4 and 5. The latter protons are suspected instead of protons 1 and 8 because of the result of the INDO calculation for 1-naphthyl radical, as discussed earlier, and also because of the experimental result obtained from 1-pyrenyl radical.

**1-Pyrenyl Radical.** The spectrum of 1-pyrenyl radical was found to have a doublet-of-doublet pattern (see Figure 8). The major doublet spacing of 18 G and the minor doublet spacing of 6 G are very close to the *ortho* and *meta* proton couplings of phenyl radical, respectively. Clearly this radical is also a  $\sigma$  type. The spectrum pattern is much simpler than that of 1-naphthyl radical. Thus one is led to conclude that most of the small structure observed with the latter radical is caused by protons 4 and 5. The smallness of the contribution to the structure by the closest proton in the neighboring ring (proton 8 in 1-naphthyl radical and proton 10 in 1-pyrenyl radical) is somewhat surprising.

The isotropic  $g$  values and hyperfine coupling constants assessed from the spectra of 1-naphthyl, 1-anthracyl, 1-pyrenyl, and 9-anthracyl radicals are compiled in Table II.

**Table II.** The Isotropic  $g$  Value and the Coupling Constants Assessed from the Spectra of 1-Naphthyl, 1-Anthracyl, 1-Pyrenyl, and 9-Anthracyl Radicals

Radical	$g$	$A$ (H <sub>2</sub> ) <sup>a</sup>	$A$ (H <sub>3</sub> ) <sup>a</sup>
1-Naphthyl	$2.002 \pm 0.0005$	$19 \pm 1$	$6.0 \pm 0.5$
1-Anthracyl	$2.002 \pm 0.0005$	$21 \pm 1$	$6.0 \pm 0.5$
1-Pyrenyl	$2.002 \pm 0.0005$	$18 \pm 0.5$	$6.0 \pm 0.5$
9-Anthracyl	$2.002 \pm 0.0005$		

<sup>a</sup> Coupling constants are given in gauss.

## Theoretical Results

**Extended Hückel Theory.** The orbital energies calculated by the extended Hückel method are summarized in Table III. As expected, these confirm the

**Table III.** Innermost Orbital Energies of Aryl Radicals Calculated from Extended Hückel Theory<sup>a</sup>

	$\pi$	$\sigma$	$\pi^*$
Phenyl	-12.8	-10.75	-8.3
1-Naphthyl	-12.1	-10.77	-9.3
2-Naphthyl	-12.1	-10.70	-9.3
9-Anthracyl	-11.6	-10.79	-9.8

<sup>a</sup> In eV (VSIP for 2p orbital on carbon = -11.4 eV).

simple qualitative considerations given in the introduction; namely, that the  $\sigma$ -orbital energy remains approximately constant while the innermost pair of  $\pi$ -orbital energies converges on a value somewhat higher (inclusion of overlap) than that of a 2p orbital on carbon. In all cases considered the  $\sigma$ -orbital energy lies between the highest occupied and lowest unoccupied  $\pi$  orbitals, in agreement with the experimental result that all are  $\sigma$

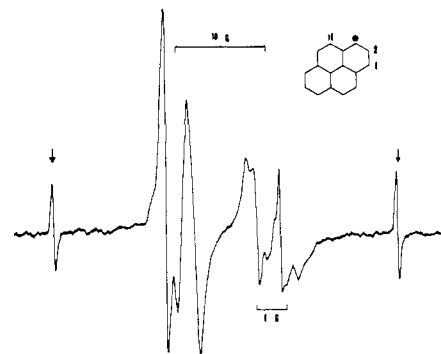
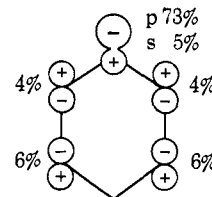


**Figure 8.** ESR spectrum of 1-pyrenyl radical in an argon matrix at 4°K. The arrows indicate the outermost components of the methyl quartet.

radicals. The  $\sigma$  orbital energy is close to the limiting value of the  $\pi$ -orbital energies, so that no level crossing would be predicted for rings considerably larger than those considered here. The LCAO coefficients of the half-filled orbital are not very sensitive to ring extension and its makeup is depicted below. It is mostly a non-



bonding p orbital in the direction of the broken bond; it contains rather little ( $\sim 5\%$ ) s character and is weakly bonding to the carbon 2p $\sigma$  orbitals in the aromatic ring. The possibility of structural distortion has not been explicitly considered.

**Self-Consistent Field.** Since the coupling constants predicted for these radicals by the extended Hückel theory generally do not agree well with the experimental values, the calculations for the phenyl and 1- and 2-naphthyl radicals were repeated using the semiempirical, unrestricted self-consistent field method of intermediate neglect of differential overlap (INDO) recently developed by Pople, Beveridge, and Dobosh.<sup>6</sup> In the present application the spin density at each atom is calculated as the difference in the diagonal elements of the density matrices for the  $\alpha$ - and  $\beta$ -spin electrons summed over the orbitals centered on the atom in question

$$\rho = R^\alpha - R^\beta \quad (1)$$

where

$$R_{\mu\mu}^\alpha = \sum_i^{\text{occ mo}} (C_{\mu i}^\alpha)^2 \quad (2a)$$

and

$$R_{\mu\mu}^\beta = \sum_i^{\text{occ mo}} (C_{\mu i}^\beta)^2 \quad (2b)$$

In eq 2 the coefficients  $C_{\mu i}$ 's are those of the orthogonalized basis set atomic orbitals  $\mu$  in the molecular orbitals  $i$ . The occupied molecular orbitals form a spin-unrestricted Slater determinant which is itself not an eigenfunction of the  $S^2$  operator but is a linear combination of eigenfunctions for the spin states of doublet and higher multiplicity. Projection of the eigenfunc-

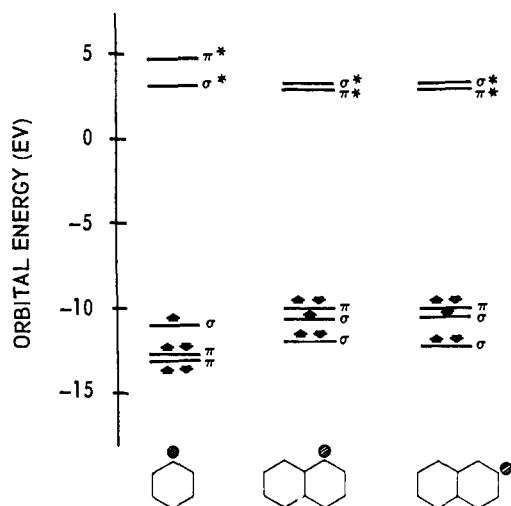


Figure 9. Innermost orbital energies of aryl radicals calculated by the INDO SCF method.

tion for the doublet state according to the method of Amos and Snyder<sup>9</sup> did not lead to any improvement in the predicted coupling constants for the phenyl radical and therefore is not included in the results presented here.

Calculations by Pople, Beveridge, and Dobosh of the proton esr coupling constants of a large number of  $\sigma$  and  $\pi$  radicals show consistently good agreement with available experimental data. Although the predicted coupling constants for the phenyl radical have already been reported,<sup>10</sup> these calculations had been done in the course of our present work, and the results along with those for the 1- and 2-naphthyl radicals are included in Table IV. As can be seen from the table, the INDO results for the proton coupling constants agree well with the experimental evidences. In fact, in the case of the 2-naphthyl radical, the calculated values have permitted a differentiation between the two *ortho*-proton coupling constants that is not possible on the basis of the available experimental evidences. The assignments made here may be considered reliable on the basis of the good agreement between theory and experiment that has been observed in other cases.

The INDO results agree with those of EHT in predicting the phenyl and the 1- and 2-naphthyl radicals to be  $\sigma$  radicals. However, INDO does predict a crossing of  $\sigma$ - and  $\pi$ -bonding molecular orbitals in going from phenyl to the naphthyl radicals, the unpaired electron

(9) A. T. Amos and L. C. Snyder, *J. Chem. Phys.*, **41**, 1773 (1964).

(10) J. A. Pople, D. L. Beveridge, and P. A. Dobosh, *J. Amer. Chem. Soc.*, **90**, 4201 (1968).

Table IV. Predicted Proton Hyperfine Coupling Constants

Radical	Proton	INDO <sup>a</sup>	EHT <sup>a</sup>	Obsd
Phenyl	<i>ortho</i>	17.85	5.80	17.5
	<i>meta</i>	5.15	2.45	6.1
	<i>para</i>	4.40	4.95	1.9
1-Naphthyl	H <sub>2</sub>	16.95	5.65	19
	H <sub>3</sub>	5.10	2.55	6
	H <sub>4</sub>	5.45	4.70	~2
2-Naphthyl	H <sub>1</sub>	16.90	5.40	15.7
	H <sub>3</sub>	18.85	5.90	19.7
	H <sub>4</sub>	4.95	2.25	5.8

<sup>a</sup> Calculated coupling constants are obtained by use of the equation  $a_H = 500\rho_H$ .

in the latter species occupying the second-highest bonding MO. These results are shown in Figure 9. The energies for the  $\alpha$ -spin and the  $\beta$ -spin orbitals do not generally have the same energy in an unrestricted SCF calculation. In spite of this, the highest occupied  $\pi$  orbitals of  $\alpha$  and  $\beta$  spin both have an energy lower than that of the unpaired  $\sigma$  orbital in the phenyl radical, whereas in the case of the naphthyl radicals both  $\pi$  molecular orbitals have a higher energy than that of the unpaired  $\sigma$  molecular orbital. For the purpose of simplifying the discussion, therefore, the  $\alpha$ - and  $\beta$ -spin molecular orbitals having the same spatial symmetry are represented in Figure 9 as one doubly occupied molecular orbital with an energy equal to the average of the values for the two different spin orbitals.<sup>11</sup>

The crossing predicted by INDO, but not by EHT, is clearly due to the explicit inclusion of electronic repulsion terms in the former. The repulsion terms should lead to upward shift of the doubly occupied bonding  $\pi$  orbital energy depicted in Figure 1 by an almost constant factor. This is not inconsistent with the EHT results that all the species considered are  $\sigma$  radicals: the  $\sigma$  MO remains singly occupied, even though it has lower energy, because of the greater repulsion that would be experienced if two electrons were to occupy this highly localized MO. This point is substantiated by considering the ordering of the levels in the 2-naphthyl radical cation. Calculations show that the radical cation in its triplet state has the singly occupied  $\pi$  MO below the singly occupied  $\sigma$  MO. Investigation of the electronic spectra of 1- or 2-naphthyl radicals should be of extreme interest, since it can directly explore the crossing of the  $\sigma$  and  $\pi$  levels predicted by the theory.

(11) The energy difference between a given  $\alpha$ -spin orbital and the corresponding  $\beta$ -spin orbital is small, never exceeding 0.2 eV in the present calculation.